JOURNAL OF BACTERIOLOGY, Aug. 2007, p. 5472–5481 Vol. 189, No. 15
0021-9193/07/$08.00+0 doi:10.1128/JB.00529-07
Copyright © 2007, American Society for Microbiology. All Rights Reserved.

CsrA Inhibits Translation Initiation of *Escherichia coli hfq* by Binding to a Single Site Overlapping the Shine-Dalgarno Sequence▽

Carol S. Baker,[1] Lél A. Eöry,[1,2]† Helen Yakhnin,[1] Jeffrey Mercante,[3] Tony Romeo,[3] and Paul Babitzke[1]*

Department of Biochemistry and Molecular Biology, The Pennsylvania State University, University Park, Pennsylvania 16802[1]; School of Biochemistry and Microbiology, University of Leeds, Leeds, United Kingdom[2]; and Department of Microbiology and Immunology, Emory University School of Medicine, Atlanta, Georgia 30322[3]

Received 6 April 2007/Accepted 18 May 2007

Csr (carbon storage regulation) of *Escherichia coli* is a global regulatory system that consists of CsrA, a homodimeric RNA binding protein, two noncoding small RNAs (sRNAs; CsrB and CsrC) that function as CsrA antagonists by sequestering this protein, and CsrD, a specificity factor that targets CsrB and CsrC for degradation by RNase E. CsrA inhibits translation initiation of *glgC*, *cstA*, and *pgaA* by binding to their leader transcripts and preventing ribosome binding. Translation inhibition is thought to contribute to the observed mRNA destabilization. Each of the previously known target transcripts contains multiple CsrA binding sites. A position-specific weight matrix search program was developed using known CsrA binding sites in mRNA. This search tool identified a potential CsrA binding site that overlaps the Shine-Dalgarno sequence of *hfq*, a gene that encodes an RNA chaperone that mediates sRNA-mRNA interactions. This putative CsrA binding site matched the SELEX-derived binding site consensus sequence in 8 out of 12 positions. Results from gel mobility shift and footprint assays demonstrated that CsrA binds specifically to this site in the *hfq* leader transcript. Toeprint and cell-free translation results indicated that bound CsrA inhibits Hfq synthesis by competitively blocking ribosome binding. Disruption of *csrA* caused elevated expression of an *hfq′-′lacZ* translational fusion, while overexpression of *csrA* inhibited expression of this fusion. We also found that *hfq* mRNA is stabilized upon entry into stationary-phase growth by a CsrA-independent mechanism. The interaction of CsrA with *hfq* mRNA is the first example of a CsrA-regulated gene that contains only one CsrA binding site.

Bacteria have evolved several regulatory strategies that ensure their survival in response to changes in their growth environment. The Csr (carbon storage regulation) and homologous Rsm (repressor of secondary metabolites) global regulatory systems of several eubacterial species control numerous genes and processes posttranscriptionally. Csr systems consist of at least one RNA binding protein that either activates or represses expression of target mRNAs, as well as one or more small noncoding regulatory RNAs (sRNAs) that contain multiple CsrA binding sites. The sRNAs function as antagonists of the RNA binding protein(s) via protein sequestration (reviewed in references 1 and 26). The Csr system of *Escherichia coli* is involved in the repression of several stationary-phase processes and the activation of some exponential-phase functions. Four major components of Csr in this organism include the homodimeric RNA binding protein CsrA, two sRNA antagonists of CsrA (CsrB and CsrC), and CsrD, a protein that specifically targets both sRNAs for degradation by RNase E (18, 35, 45). CsrA represses gluconeogenesis, glycogen metabolism, peptide transport, and biofilm formation (11, 16, 27, 28, 42, 48), while it activates glycolysis, acetate metabolism, and flagellum biosynthesis (28, 43, 44). CsrB and CsrC sequester CsrA and prevent its interaction with mRNA targets. Multiple imperfect repeat sequences in these regulatory RNAs function as CsrA binding sites, such that each sRNA is capable of sequestering several CsrA dimers (14, 18, 45).

CsrA negatively regulates expression of the glycogen biosynthetic gene *glgC* by binding to four sites in the untranslated leader of the *glgCAP* operon transcript, one of which overlaps the *glgC* Shine-Dalgarno (SD) sequence (reference 2 and unpublished results). CsrA binding to the *glgCAP* leader transcript inhibits GlgC synthesis by blocking ribosome binding. Presumably, CsrA-mediated inhibition of *glgC* translation is responsible for the accelerated rate of *glgCAP* mRNA decay (19). CsrA also represses translation of *cstA*, a carbon starvation-induced gene thought to be involved in peptide transport (11, 31), as well as the first gene in the *pgaABCD* operon, a cluster of genes that are required for the synthesis of the polysaccharide adhesin poly-β-1,6-*N*-acetyl-D-glucosamine (PGA), which participates in biofilm formation (42). CsrA binds to four sites in the *cstA* transcript and to six sites in the *pga* operon leader transcript. In each case, one of the CsrA binding sites overlaps the cognate SD sequence. Translational repression of these genes proceeds by a mechanism that is similar to the mechanism identified for *glgC* (11, 42). Considerable sequence variation exists among the known *E. coli* CsrA binding sites; however, GGA is a highly conserved sequence element which is often present in the loop of short RNA hairpins. Systematic evolution of ligands by exponential enrichment (SELEX) was used to isolate high-affinity CsrA ligands (10). The high-affinity RNA ligands contained a single CsrA

* Corresponding author. Mailing address: Department of Biochemistry and Molecular Biology, The Pennsylvania State University, University Park, PA 16802. Phone: (814) 865-0002. Fax: (814) 863-7024. E-mail: pxb28@psu.edu.

† Present address: Institute of Evolutionary Biology, School of Biological Sciences, University of Edinburgh, Edinburgh, United Kingdom.

▽ Published ahead of print on 25 May 2007.

binding site with a consensus sequence of RUACARGGA UGU, with the underlined residues being 100% conserved. In each case the GGA motif was present in the loop of a short predicted hairpin (10).

A bioinformatics approach was used to search the *E. coli* genomic database for genes containing potential CsrA binding sites. A potential CsrA binding site was identified that overlaps the *hfq* SD sequence, suggesting that CsrA might regulate translation initiation of this gene. *E. coli* Hfq is a toroid-shaped homohexamer that was discovered as a protein required for in vitro transcription of bacteriophage Qβ RNA (12, 29). Hfq is present in a wide range of bacterial species, and its role in global control of gene expression is readily apparent, as it impacts numerous physiological processes, such as virulence, bacteriocin production, and nitrogen fixation (40). Numerous studies have established that Hfq functions as an RNA chaperone in promoting sRNA-mRNA base-pairing (reviewed in references 13 and 34). For example, it is well established that Hfq activates translation of σS, the stationary-phase sigma factor, by promoting base-pairing of two sRNAs to the *rpoS* leader transcript. Base-pairing of either sRNA disrupts an inhibitory RNA structure in the *rpoS* leader such that translation is stimulated (13, 23, 34).

We confirmed that CsrA binds to the site in *hfq* identified in silico. As this CsrA binding site overlaps the *hfq* SD sequence, bound CsrA inhibits translation initiation of *hfq* by blocking ribosome binding. The interaction of CsrA with the *hfq* transcript described here is unique, as this is the first example of a CsrA-regulated mRNA that contains only a single CsrA binding site. Because Hfq mediates many intermolecular sRNA-mRNA interactions in the cell, these findings imply that CsrA has a substantially greater influence on global regulatory networks than previously recognized.

MATERIALS AND METHODS

Bacterial strains and plasmids. Plasmid pCSB52 contains the wild-type *hfq* leader and the first 55 nucleotides (nt) of the *hfq* coding region (+1 to +124 relative to the start of $P3_{hfq}$ promoter transcription) (37) cloned into the pTZ18U polylinker (United States Biochemical Corp.). pCSB60 contains an *hfq'-'lacZ* translational fusion consisting of the $P3_{hfq}$ promoter and leader region as well as the first 18 codons of *hfq* (−66 to +124 relative to the start of $P3_{hfq}$ transcription), cloned in frame with the *lacZ* gene of pMLB1034 (32). Three nucleotide substitutions in the *hfq* leader just upstream of the SD sequence and within the CsrA binding site (A51T:T52G:A53C) were introduced into pCSB60 using the QuikChange II protocol (Stratagene), resulting in plasmid pCSB62. *E. coli* strains used for β-galactosidase assays were constructed to create single-copy chromosomal gene insertions of *hfq'-'lacZ* translational fusions into the λ *att* site using the λInCh protocol as described previously (5). Strains PLB785 and PLB786 contain the *hfq'-'lacZ* fusion from pCSB60 integrated into the chromosome of strains CF7789 (MG1655 Δ*lacI-Z* [MluI]) and TR1-5CF7789 (CF7789 *csrA::kan*), respectively. Strains PLB923 and PLB924 contain the *hfq'-'lacZ* fusion from pCSB62 integrated into the chromosomes of CF7789 and TR1-5CF7789, respectively. Plasmid pCRA16 (36) contains *csrA* cloned into pBR322 (4). Strain PLB786 was transformed with pBR322 and pCRA16 to generate strains PLB789 and PLB793, respectively. Plasmid pYH109 was generated by replacing the *Bacillus subtilis trp* operon sequence in pYH28 (30) with a PCR fragment containing the *hfq* leader and amino-terminal coding sequence (+1 to +179 relative to $P3_{hfq}$ transcription), resulting in an *hfq'-'gfp* translational fusion (37th *hfq* codon fused in frame with *gfp*). The *E. coli smpB* gene was cloned into the pET28A$^+$ polylinker (Novagen) to create pETB. Unless otherwise indicated, all strains were grown at 37°C in Lennox LB medium. When appropriate, growth media were supplemented with antibiotics to the following concentrations: ampicillin, 100 μg/ml; kanamycin, 50 μg/ml; tetracycline, 20 μg/ml.

Gel mobility shift assay. Quantitative gel mobility shift assays followed a previously published procedure (46). *E. coli* CsrA-H6 protein was purified as described previously (10). RNA was synthesized in vitro using the MEGAscript kit (Ambion) and linearized pCSB52 as template. Gel-purified RNA was 5′-end labeled with [γ-^{32}P]ATP as described previously (46). RNA suspended in Tris-EDTA (TE) buffer was renatured by heating to 80°C followed by slow cooling to room temperature. Binding reaction mixtures (10 μl) contained 10 mM Tris-HCl, pH 7.5, 10 mM $MgCl_2$, 100 mM KCl, 32.5 ng of yeast RNA, 7.5% glycerol, 20 mM dithiothreitol (DTT), 4 U of RNase inhibitor (Promega), 0.5 nM *hfq* leader RNA, purified CsrA-H6 (various concentrations), and 0.1 mg/ml xylene cyanol. Competition assay mixtures also contained unlabeled RNA competitor. Reaction mixtures were incubated for 30 min at 37°C to allow CsrA-RNA complex formation. Samples were then fractionated on native 8% polyacrylamide gels. Radioactive bands were visualized with a phosphorimager. Free and bound RNA species were quantified using ImageQuant (Molecular Dynamics), and the apparent equilibrium binding constant (K_d) of the CsrA-*hfq* RNA interaction was calculated as described previously (46).

Toeprint assay. Toeprint assays were performed by modifying published procedures (2, 15). *hfq* leader transcripts used in this analysis were synthesized using the MEGAscript kit and linearized pCSB52 as template. Gel-purified *hfq* leader RNA (500 nM) in TE was renatured and hybridized to a 5′-end-labeled DNA oligonucleotide (500 nM) in TE that was complementary to the 3′ end of the transcript. Hybridization was accomplished by heating the mixture to 80°C followed by slow cooling to room temperature. Toeprint assay mixtures contained various concentrations of CsrA-H6 and/or 260 nM 30S ribosomal subunits and 5 μM $tRNA^{fMet}$. *E. coli* ribosomes were purified as described previously (25). Purified 30S ribosomal subunits were obtained by denaturing 70S ribosomes, followed by purification through a sucrose gradient. 30S subunit fractions were pooled and stored at −80°C in 10 mM Tris-HCl, pH 7.5, 60 mM NH_4OAc, 6 mM 2-mercaptoethanol, 10 mM $MgCl_2$, and 10% glycerol. Previously frozen 30S ribosomal subunits were thawed, activated by incubation at 37°C for 15 min, and kept on ice until addition to toeprint reaction mixtures. Toeprint reaction mixtures (20 μl) contained 2 μl of the hybridization mixture, 375 μM each deoxynucleoside triphosphate, and 10 mM DTT in toeprint buffer (10 mM Tris-HCl, pH 7.4, 10 mM $MgCl_2$, 60 mM NH_4OAc, 6 mM 2-mercaptoethanol). Mixtures containing CsrA were incubated for 30 min at 37°C to allow CsrA-mRNA complex formation. 30S ribosomal subunit toeprint reactions were performed by incubating RNA, 30S ribosomal subunits, and $tRNA^{fMet}$ in toeprint buffer as described previously (15). Following the addition of 3 U of avian myeloblastoma virus reverse transcriptase (Roche), the reaction mixture was further incubated for 15 min at 37°C. Reactions were terminated by the addition of 12 μl of stop solution (70 mM EDTA, 85% formamide, 0.1× Tris-borate-EDTA, 0.025% xylene cyanol, and 0.025% bromophenol blue). Samples were heated at 95°C for 5 min prior to fractionation through standard 6% polyacrylamide sequencing gels. Sequencing reactions were performed using pCSB52 as the template and the same end-labeled DNA oligonucleotide as a primer. Radioactive bands were visualized with a phosphorimager.

RNA footprint assay. Preparation of 5′-end-labeled *hfq* leader transcripts was as described for the gel shift analysis. Titrations of RNase T_1 (Roche) and RNase T_2 (Sigma) were performed to identify the amount of enzyme in which ~90% of the transcripts were full length to minimize multiple cleavages in any one transcript. Binding reaction mixtures (10 μl) containing various concentrations of CsrA-H6 and 50 nM *hfq* RNA were otherwise identical to those described for the gel shift assay. After the initial binding of CsrA-H6, either RNase T_1 (0.025 U) or RNase T_2 (0.03 U) was added to the reaction mixtures, and incubation was continued for 15 min at 37°C. Reactions were terminated by the addition of 10 μl of gel loading buffer II (Ambion) and kept on ice. Partial alkaline hydrolysis and RNase T_1 digestion ladders of each transcript were prepared as described previously (3). Samples were fractionated through standard 6% polyacrylamide sequencing gels. Radioactive bands were visualized with a phosphorimager.

β-Galactosidase assays. Bacterial cultures growing in liquid medium at 37°C were monitored using a Klett-Summerson colorimeter (no. 52 green filter). Culture samples (4 ml) were harvested at various times, washed once with 10 mM Tris-HCl, pH 7.5, and frozen as cell pellets at −20°C. Cell extracts were prepared by suspending frozen cell pellets in 0.5 ml of BugBuster protein extraction reagent (Novagen), followed by incubation at 37°C in an air shaker. After 30 min, 0.3 ml of Z buffer (24) containing 0.2 mg/ml lysozyme was added to each sample, and incubation was continued for 30 min at 37°C in an air shaker. Cell debris was removed by centrifugation at 4°C. β-Galactosidase assays were performed using the cell extracts (2, 24). Protein concentrations were determined by the Bio-Rad protein assay with bovine serum albumin as a standard.

mRNA abundance and mRNA half-life assays. Bacterial cultures were mixed with 2 volumes of RNAprotect bacterial reagent (QIAGEN) and incubated at room temperature for 5 min. Cells were then harvested, and total RNA was prepared using the Masterpure RNA purification kit (Epicenter) and treated

with DNase I according to the manufacturer's recommendations. RNA was quantified by measuring the absorbance at 260 and 280 nm.

To measure *hfq* transcript levels, strains MG1655 (wild type) and TR1-5MG1655 (*csrA::kan*) were grown at 37°C in Lennox LB medium to exponential phase (optical density at 600 nm of 0.4) or to early stationary phase (optical density at 600 nm of 4.0). Total RNA was purified, and the steady-state level of *hfq* mRNA was determined by real-time quantitative reverse transcription-PCR (RT-qRT-PCR) using the primer pair hfq-Fw (5′-AAGCACGCGATTTCTAC TGTTG-3′) and hfq-Rv (5′-CCACCGGCGTTGTTACTGT-3′) and the probe Hfq-6FAM-BHQ1 (5′-CCCGTCTCGCCCGGTTTCTCA-3′), which was 5′-end labeled with 6-carboxyfluorescein (6FAM) and 3′-end labeled with Black Hole Quencher 1 (BHQ1). RT-qRT-PCR was performed using the iScript one-step RT-PCR kit for probes (Bio-Rad) with a Bio-Rad iCycler IQ real-time system. The conditions used for RT-PCR were as follows: 50°C for 10 min, 95°C for 5 min, and 40 cycles of 95°C for 15 s and 65°C for 30 s. Unless otherwise noted, all primers and probes were used at a final concentration of 200 nM. Real-time measurements were taken during the 65°C step. Reactions were performed in triplicate in two independent experiments, each time with 100 ng of template RNA. A set of reactions lacking reverse transcriptase was performed for each RNA sample as a control for DNA contamination. For normalization of *hfq* RNA levels, RT-qRT-PCRs were performed with each sample for 16S rRNA quantitation using the primer pair 16S-Fw (5′-CGTGTTGTGAAATGTTGGG TTAA-3′) and 16S-Rv (5′-CCGCTGGCAACAAAGGATA-3′) and the probe 16S-6FAM-BHQ1 (5′-TCCCGCAACGAGCGCAACC-3′). The reaction conditions for RT-qRT-PCR of 16S rRNA were identical to *hfq* except that 1 ng of RNA template was used for each reaction. The $2^{-\Delta\Delta CT}$ method was used to calculate relative *hfq* RNA levels, which allowed for the use of a 16S rRNA control (20).

For *hfq* mRNA half-life studies, strains MG1655 (wild type) and TR1-5MG1655 (*csrA::kan*) were grown as described above. Cells were harvested at various times following the addition of rifampin (200 μg/ml final concentration), and total RNA was purified as described above using RNAprotect. RT-qRT-PCR was performed as described above for steady-state *hfq* RNA determinations. The percentage of RNA remaining through the time course was determined by calculating the difference in cycle threshold (ΔC_T) and the subsequent fold difference compared to the 0-min time point after controlling for 16S rRNA levels.

RNA-directed cell-free translation. Cell-free translation reactions followed previously published procedures (9, 47). Transcripts for this analysis were synthesized using the Ambion MEGAscript kit. *hfq′-′gfp* and *smpB* transcripts were synthesized using linearized pYH109 and pETB as templates, respectively. *bla* was transcribed from a 1,020-nt PCR fragment containing a T7 promoter. CsrA-deficient *E. coli* S-30 extract was prepared from TR1-5 MG1655 (*csrA::kan*) according to published procedures (47). The S-30 extract was preincubated with RNase-free DNase I for 15 min at 37°C to remove chromosomal DNA and to allow time for *E. coli* RNases to degrade endogenous mRNA. Reaction mixtures (24 μl) contained 60 mM Tris-HEPES, pH 7.5, 60 mM NH_4Cl, 5 mM to 15 mM $MgCl_2$ (determined empirically for each transcript), 12 mM KCl, 0.5 mM EGTA, 5 mM DTT, 2 mM ATP, 0.6 mM GTP, 0.08 mM calcium folinate, 4 mg/ml of aprotinin, 4 mg/ml of leupeptin, 4 mg/ml of pepstatin A, 4 μl S-30 extract (12 mg of total protein), 800 U/ml of DNase I, 500 U/ml of RNasin, 10 mM phosphoenolpyruvate, 35 U of pyruvate kinase, 0.4 mg/ml of *E. coli* tRNA, 0.04 μg/ml of mRNA, 10 μCi [^{35}S]methionine, 0.5 mM of each of the other amino acids, and 0.8 mM spermidine. Reaction mixtures were incubated for 45 min at 37°C and terminated by adding 6 μl of stop buffer (125 mM Tris-HCl, pH 6.8, 5% sodium dodecyl sulfate [SDS], 25% glycerol, 2% 2-mercaptoethanol, and 12.5 mg/ml of bromophenol blue). Samples were heated at 95°C for 5 min prior to fractionation by 14% SDS-polyacrylamide gel electrophoresis (PAGE). Radioactive bands were visualized with a phosphorimager and quantified using ImageQuant.

RESULTS

Identification of *hfq* as a potential CsrA-regulated gene. A genome search program was developed to identify potential CsrA binding sites by exploring the properties of known CsrA binding motifs. A total of 14 CsrA binding sites were previously identified in the leader regions of *glgC*, *cstA*, and *pgaA* (references 2, 11, and 42 and unpublished results). These sequences were aligned using ClustalW (7), and a position weight matrix (pwm) was calculated from the alignment using the MATCH tool (17). The pwm was then used as a scoring function to identify potential CsrA binding sites within the *E. coli* genomic database. The scores were assigned from 0 to 100% according to the minimum and the maximum score calculated from the pwm. The details of the pwm will be published elsewhere. This program predicted the presence of CsrA binding sites in 278 genes with scores of 96.5% or above, including the three genes that were used in generating the pwm (*cstA*, *glgC*, and *pgaA*). A CsrA binding site with a score of 96.8% was identified that overlaps the *hfq* SD sequence. This predicted sequence also conformed to the SELEX-derived consensus sequence in 8 out of 12 positions (Fig. 1). However, unlike the CsrA binding sites identified by SELEX, secondary structural predictions using MFOLD (49) indicated that the GGA motif within this putative CsrA binding site was not present in the loop of a hairpin. The pwm also identified three potential sites with scores between 81.8 and 83.5%; however, since all three of these sites overlapped the predicted site with a score of 96.8% and none of them contained an appropriately positioned GGA motif, it appeared that *hfq* contained one likely CsrA binding site. Because all of the known CsrA-controlled genes contained four to six CsrA binding sites, experiments were carried out to determine whether *hfq* contained a single CsrA binding site and whether CsrA could bind to this site in *hfq* and regulate its expression.

FIG. 1. Predicted CsrA binding site overlapping the *hfq* SD sequence. The SELEX-derived CsrA binding site consensus sequence is shown above the predicted CsrA binding site in *hfq* mRNA. Vertical lines mark the residues in the predicted site that match those in the consensus. Positions of the *hfq* SD sequence and translation initiation codon (Met) are shown.

CsrA binds to the predicted site in *hfq*. *hfq* transcription is driven by three promoters just upstream of its coding sequence. The *hfq* transcript originating from the SD sequence-proximal P3 promoter ($P3_{hfq}$) contains a 68-nt untranslated leader (37). To characterize the interaction of CsrA with *hfq* RNA, quantitative gel mobility shift assays were performed with an *hfq* transcript containing nucleotides +1 to +124 relative to the start of $P3_{hfq}$ transcription. Since quantitative gel mobility shift assays using native CsrA or C-terminal His-tagged CsrA (CsrA-H6) did not show any significant difference in binding affinities for target transcripts (data not shown), CsrA-H6 was used in all in vitro assays and is referred to as CsrA from here on. CsrA bound to this *hfq* transcript as a distinct band in native gels between 4 and 512 nM CsrA (Fig. 2A). A complete shift was observed at 128 nM CsrA, and no additional shifted species of higher molecular weights were observed as the concentration of CsrA was increased further, suggesting that CsrA binds to a single site in the *hfq* leader transcript. A nonlinear least-squares analysis of these data yielded an estimated K_d value of 38 ± 13 nM CsrA (mean ± standard deviation). For comparison, the affinities of CsrA for *glgC* (four CsrA binding sites), *cstA* (four CsrA binding sites), and *pgaA* (six CsrA binding sites) were 39 nM, 40 nM, and 22 nM, respectively (2, 11, 42).

The specificity of the CsrA-*hfq* RNA interaction was inves-

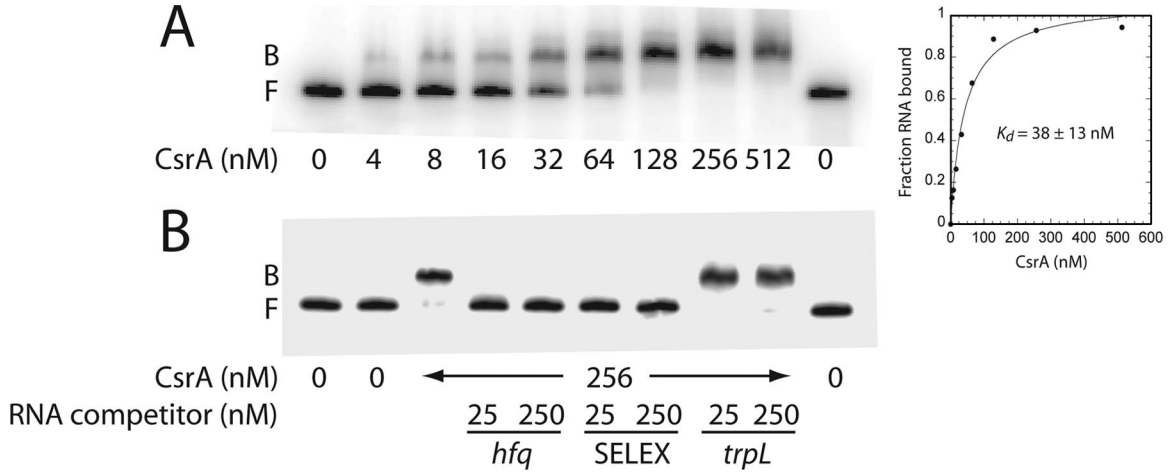

FIG. 2. Gel mobility shift analysis of the CsrA-*hfq* RNA interaction. 5′-end-labeled *hfq* RNA was incubated with the concentration of CsrA shown at the bottom of each lane. Gel shift assays were performed in the absence (A) or presence (B) of various unlabeled competitor RNAs. The concentration of each competitor RNA is shown at the bottom of each lane in panel B. The positions of bound (B) and free (F) *hfq* RNA are shown at the left of each gel. (A) Determination of the equilibrium binding constant of the CsrA-*hfq* RNA interaction. The simple binding curve for these data is shown at the right. (B) Competition assay for the CsrA-*hfq* RNA interaction to establish binding specificity. Lanes corresponding to competition with specific (*hfq* and SELEX) and nonspecific (*trpL*) RNAs are indicated.

tigated by performing competition experiments with specific (*hfq* leader and a SELEX-derived ligand) and nonspecific (*Bacillus subtilis trp* leader) unlabeled RNA competitors (Fig. 2B). Unlabeled *hfq* and SELEX transcripts were effective competitors, whereas the *B. subtilis trp* leader RNA (*trpL*) did not compete with the CsrA-*hfq* RNA interaction. These results establish that CsrA binds specifically to *hfq* RNA.

CsrA-*hfq* RNA footprint experiments were conducted to identify the position of bound CsrA in the *hfq* transcript. Single-strand-specific RNases were used as probes for these studies. As the concentration of CsrA was increased from 0 to 2 μM, protection of several nucleotides from RNase T_1 (G specific) and RNase T_2 (A preference) cleavage was observed (Fig. 3A). CsrA protected G49, G57, and G58 from RNase T_1 cleavage, as well as residues A51 through A61 from RNase T_2 cleavage. Importantly, the entire sequence overlapping the *hfq* SD sequence identified in silico was protected from RNase cleavage. The composite footprint indicates that CsrA protects one RNA segment extending from G49 through A61 (Fig. 3B). Previous RNA structure mapping identified two stable RNA hairpins in the *hfq* transcript (h1 and h2) (41). The presence of these hairpins was confirmed; residues corresponding to h1 and h2 were protected from RNase cleavage in the absence of bound CsrA (Fig. 3). Bound CsrA also resulted in increased RNase T_2 cleavage of C20 and C42. These two residues are located within the 5′ side bulge of h1 and just downstream of h1, respectively. CsrA-dependent protection was also observed for residues A76 (RNase T_2), G77 (RNase T_1), and G78 (RNase T_1). These residues are present within the stem of a predicted RNA hairpin containing a GNRA tetraloop (ΔG, −4.0 kcal/mol) (22, 49). Thus, it appears that bound CsrA stabilizes this structure (Fig. 3).

Bound CsrA inhibits translation initiation of *hfq*. Primer extension inhibition (toeprint) experiments were performed to determine whether CsrA was capable of competing with 30S ribosomal subunits for binding to the *hfq* transcript. The presence of bound CsrA or 30S ribosomal subunits should stop primer extension by reverse transcriptase, resulting in a toeprint band near the 3′ boundary of the bound macromolecule. Stable secondary structures are also capable of inhibiting extension by reverse transcriptase, resulting in a toeprint band near the 3′ end of the RNA hairpin. The toeprint results are presented in Fig. 4 and summarized in Fig. 3B. The presence of CsrA resulted in toeprints at positions A43, A82, and A91. The toeprint at A91 provides additional evidence for the hairpin containing the GNRA tetraloop, as this structure ends at A89 (Fig. 3B). The toeprint at A43 likely corresponds to the base of h1, as this RNA hairpin ends at G39. The origin of the A82 toeprint is unclear, as it is not near the 3′ end of a stable hairpin and is 21 nt downstream from the 3′ end of the CsrA footprint (Fig. 3 and 4). Since a toeprint corresponding to the 3′ boundary of bound CsrA was not observed, it appears that reverse transcriptase is effective at displacing CsrA when bound to a single site.

Toeprint assays were also performed to identify the positions of bound 30S ribosomal subunits. A prominent $tRNA^{fMet}$-dependent 30S ribosomal subunit toeprint band was observed 15 nt down from the A of the AUG initiation codon, which is the same distance from the translation initiation codon as was previously observed for several mRNAs (2, 11, 42, 47). The second 30S ribosomal subunit-dependent toeprint at G72 was not expected, and its origin is unknown. Toeprint experiments were also carried out to determine whether bound CsrA could inhibit ribosome binding. Importantly, when CsrA was bound to the *hfq* transcript prior to the addition of 30S ribosomal subunits and $tRNA^{fMet}$, each of the CsrA-dependent toeprint bands was observed, whereas the 30S ribosomal subunit toeprint bands were eliminated (Fig. 3B and 4). Thus, our toeprinting results demonstrate that bound CsrA prevents ribosome binding to the *hfq* transcript, suggesting that CsrA could be capable of preventing translation initiation and Hfq synthesis.

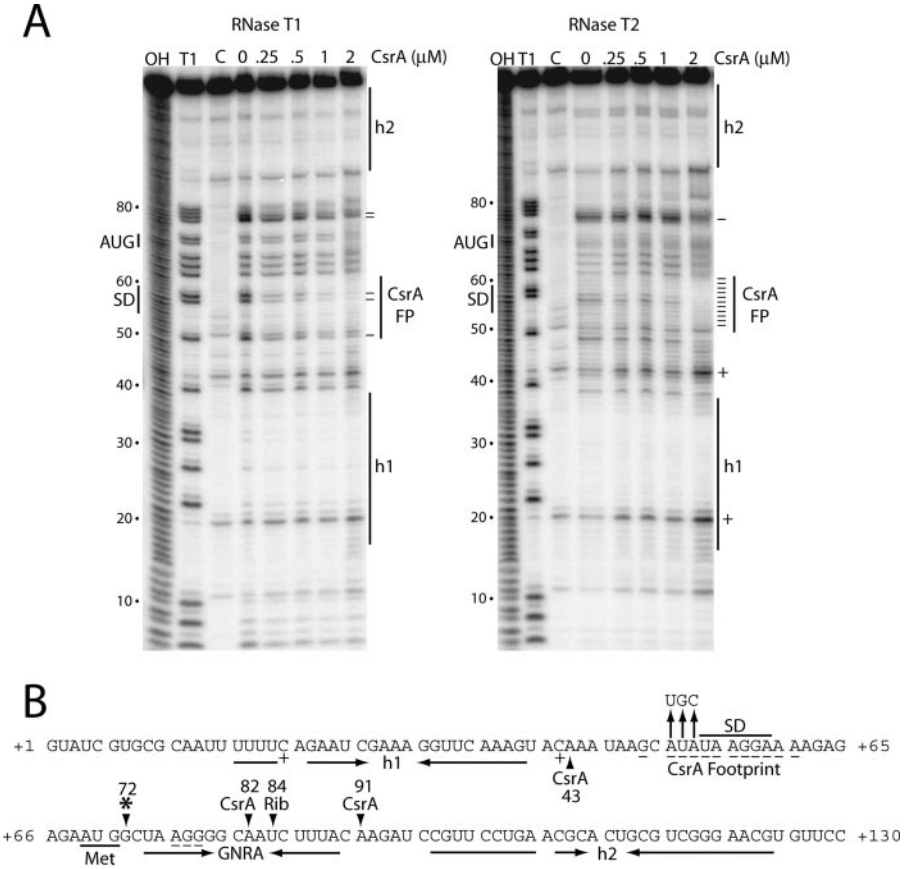

FIG. 3. CsrA-*hfq* RNA footprint analysis. (A) *hfq* RNA was treated with RNase T_1 or RNase T_2 in the absence or presence of CsrA. The concentration of CsrA used is indicated at the top of each lane. Partial alkaline hydrolysis (OH) and RNase T_1 digestion (T_1) ladders, as well as control (C) lanes in the absence of RNase treatment, are shown. The RNase T_1 ladder was generated under denaturing conditions so that every G residue in the transcript could be visualized. Residues in which RNase cleavage was reduced (−) or enhanced (+) in the presence of CsrA are marked. The positions of the CsrA footprint (FP), the *hfq* SD sequence, and the translation initiation codon (AUG) are shown. Two RNA segments corresponding to RNA secondary structures (h1 and h2) that were previously identified are shown (41). Numbering at the left of each gel is from the start of *hfq* transcription. (B) Summary of the *hfq* footprint results (from panel A) and toeprint results (from Fig. 4, below). The composite CsrA footprint shows the residues in which cleavage was reduced (−) or enhanced (+) by the presence of bound CsrA. Residues corresponding to the CsrA-dependent and 30S ribosomal subunit (Rib) toeprints are marked with arrowheads. An additional 30S ribosomal subunit-dependent toeprint is marked (*). The positions of the *hfq* SD sequence and translation initiation codon (Met) are indicated. Inverted horizontal arrows identify the residues corresponding to h1, h2, and a short RNA hairpin containing a GNRA tetraloop. Vertical arrows identify a triple nucleotide substitution introduced into the CsrA binding site. Numbering is from the start of *hfq* transcription.

Since our in vitro binding studies demonstrated that bound CsrA blocks ribosome binding, RNA-directed cell-free translation experiments were conducted to determine whether CsrA inhibits Hfq synthesis (Fig. 5). Our initial attempt to examine the effect of CsrA on Hfq synthesis was problematic, as we observed multiple bands, suggesting that hexameric Hfq was not completely denatured (data not shown). Because we previously found that using *gfp* translational fusions circumvented similar problems in cell-free translation experiments with *B. subtilis* S-30 extracts, an *hfq′-′gfp* translational fusion transcript was tested in the *E. coli* S-30 extract. In this case, well-behaved Hfq-Gfp fusion polypeptides were produced that migrated as a doublet. Importantly, addition of increasing concentrations of CsrA to the cell-free translation system led to a corresponding decrease in the Hfq-Gfp synthesis (Fig. 5). Similar cell-free translation experiments were carried out using *smpB* and *bla* transcripts as negative controls. The *smpB* transcript contained an SD sequence derived from pET28A$^+$, whereas the *bla* transcript contained its natural SD sequence. Slight CsrA-dependent translation inhibition was observed for the negative controls, although the level of inhibition was far less than for Hfq-Gfp (Fig. 5). These results, in conjunction with the in vitro binding studies, demonstrate that CsrA inhibits translation initiation of *hfq* by blocking ribosome access to the *hfq* transcript.

As Hfq was previously shown to repress its own translation (41), it was of interest to determine whether CsrA- and Hfq-mediated translation control is additive. Results from cell-free translation experiments confirmed that Hfq represses its own translation (Fig. 5C and data not shown). Moreover, an additive effect of CsrA and Hfq on translation inhibition was observed at protein concentrations of ≥0.8 μM (Fig. 5C). This latter result was somewhat surprising, as one of the Hfq binding sites overlaps the single CsrA binding site.

CsrA inhibits *hfq* expression. CsrA-dependent regulation of *hfq* was examined in vivo using an *hfq′-′lacZ* translational fusion whose expression was driven by $P3_{hfq}$ (37). This fusion was

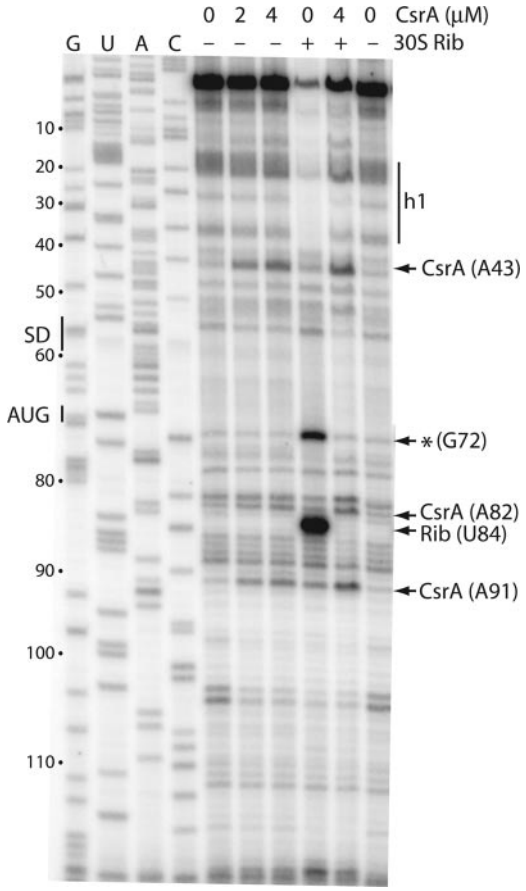

FIG. 4. CsrA and 30S ribosomal subunit toeprint analysis of *hfq* RNA. The concentration of CsrA used in each reaction mixture, as well as the absence (−) or presence (+) of $tRNA^{fMet}$ and 30S ribosomal subunits (30S Rib), is shown at the top of each lane. CsrA was added prior to 30S ribosomal subunits when both were present in the same reaction mixture. Arrows identify CsrA-dependent and 30S ribosomal subunit (Rib) toeprint bands. An additional 30S ribosomal subunit-dependent toeprint is marked (∗). Positions of the *hfq* SD sequence and the translation initiation codon (AUG) are shown. The RNA segment corresponding to h1 is also shown. Sequencing lanes to reveal G, U, A, or C residues are marked. Numbering is from the start of *hfq* transcription.

integrated into the lambda *att* site of the *E. coli* chromosome in single copy, and expression was examined throughout the growth curve in both wild-type and *csrA* mutant backgrounds. When compared to the wild-type strain, a small but reproducible increase in expression (~30%) was observed in the *csrA* mutant during stationary-phase growth (Fig. 6A). Expression was also examined when cells were grown in LB plus 1% glucose, because we previously found that expression of a *cstA'-'lacZ* fusion in wild-type and mutant strains differed to a greater extent under this glycolytic growth condition (11). A somewhat higher increase in expression (~50%) was observed in the *csrA* mutant from the late exponential to the stationary phase of growth when cells were grown in LB plus 1% glucose (Fig. 6C). Introduction of *csrA* on a plasmid complemented the *csrA* mutant defect, resulting in a twofold reduction of *hfq'-'lacZ* expression beginning in late exponential phase (Fig. 6B).

We attempted to examine the influence of a mutant CsrA binding site on *hfq* expression. Because the critical GGA motif in this binding site is part of the *hfq* SD sequence, three CsrA binding site residues located just upstream from the *hfq* SD sequence were altered (A51T:T52G:A53C) (Fig. 3B). Expression from this mutant fusion was reduced ~5-fold in both wild-type and *csrA* mutant strains (Fig. 6C), suggesting that sequence alterations this close to the SD sequence had deleterious effects on translation initiation. Furthermore, it is apparent that these substitutions did not eliminate CsrA-dependent inhibition of *hfq* expression, suggesting that a more substantial change to the CsrA binding site would be needed to prevent the CsrA-*hfq* RNA interaction. While the reason for reduced translation of the binding site mutant is not known, RNA secondary structure predictions using MFOLD (49) suggest that RNA structural rearrangements are not the cause.

Previous studies established that the mRNAs of several CsrA-repressed genes were stabilized in *csrA* mutant strains (1, 26). The steady-state level of *hfq* mRNA was determined by RT-qRT-PCR in wild-type and *csrA* mutant strains in the exponential and early stationary phases of growth. The relative abundance of *hfq* mRNA was 2-fold and 1.7-fold higher in the *csrA* mutant strain during exponential and early stationary phases of growth, respectively. The increased level of *hfq* mRNA in the *csrA* mutant strain could have been caused by increased transcription or a reduction in the mRNA decay rate. Results from mRNA half-life experiments indicated that CsrA does not affect the stability of *hfq* mRNA, suggesting that CsrA indirectly influences *hfq* transcription (Fig. 7). While the half-life of *hfq* mRNA was similar in wild-type and *csrA* mutant strains, we found that *hfq* transcripts were dramatically stabilized in the early stationary phase of growth (Fig. 7). Thus, it appears that mRNA stabilization contributes to increased *hfq* expression in stationary phase by a CsrA-independent mechanism.

DISCUSSION

CsrA is a global regulatory RNA binding protein that represses or activates gene expression posttranscriptionally. Bound CsrA inhibits expression of several genes by binding to multiple sites within target transcripts, one of which overlaps the cognate SD sequence, thereby blocking ribosome binding. Inhibition of translation is thought to contribute to the observed accelerated rate of mRNA decay (1, 26). In the case of gene activation, bound CsrA can stabilize target transcripts, although the mechanism of message stabilization is not known (43). Two sRNA antagonists of CsrA, CsrB and CsrC, contain multiple CsrA binding sites and function by sequestering this protein (18, 45). Expression of *csrA*, *csrB*, and *csrC* increases as the culture approaches stationary phase (14, 45). The BarA/UvrY two-component signal transduction system activates transcription of *csrB* and *csrC* (36). Although the signal for this activation is not known, BarA signaling appears to be pH dependent (21). Interestingly, CsrA indirectly activates synthesis of both of the sRNAs via the response regulator UvrY, resulting in an autoregulatory circuit for CsrA, CsrB, and CsrC (36, 45). A fourth Csr component, the CsrD protein, was recently shown to be a specificity factor that targets CsrB and CsrC for degradation by RNase E (35). As CsrA acts downstream of transcriptional regulation and generally affects gene

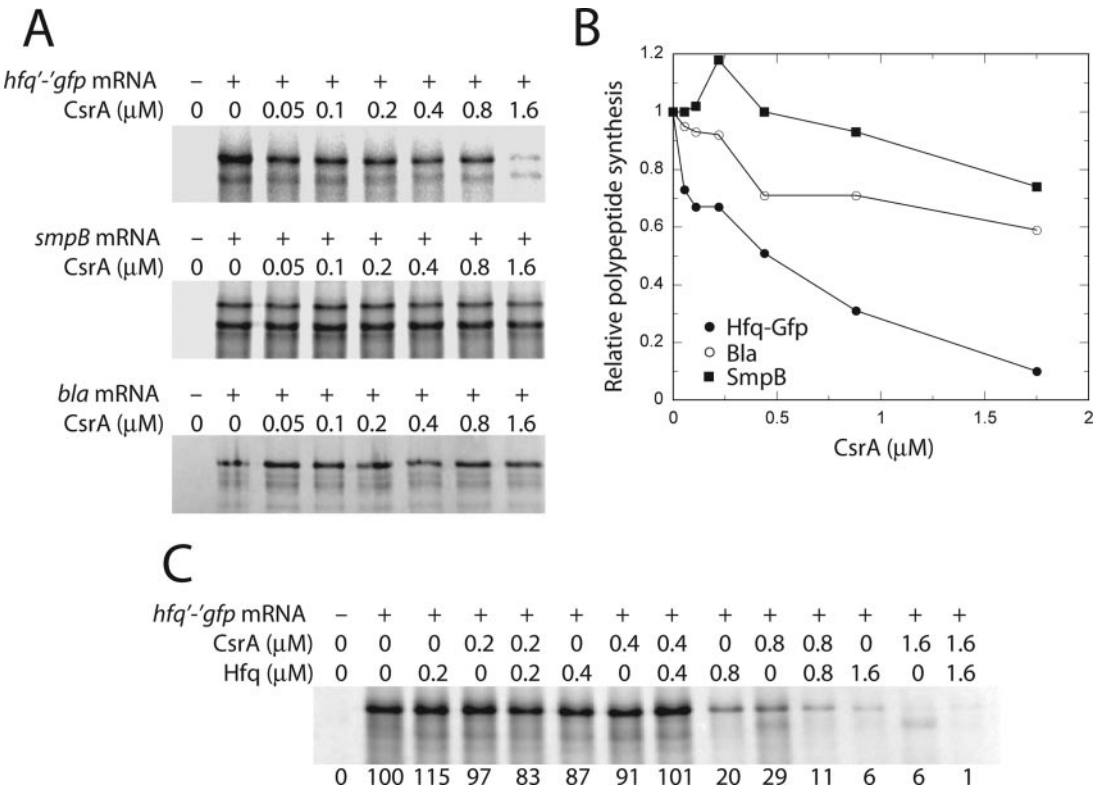

FIG. 5. Effect of CsrA and Hfq on in vitro translation of *hfq'-'gfp* mRNA. The *E. coli* S-30 extract was prepared from a CsrA-deficient strain. (A) Reactions were carried out with the concentration of CsrA indicated at the top of each lane in the absence (−) or presence (+) of *hfq'-'gfp* or control (*smpB* or *bla*) transcripts. Hfq-GFP, SmpB, and Bla translation products were analyzed by SDS-PAGE. (B) Relative levels of Hfq-GFP, SmpB, and Bla polypeptide synthesis as a function of CsrA concentration. All of the bands shown in panel A were used for quantifying the effect of CsrA on protein synthesis. The level of polypeptide synthesis in the absence of CsrA was set to 1.0 for each transcript. (C) Reactions were carried out with the concentration of CsrA and/or Hfq indicated at the top of each lane in the absence (−) or presence (+) of *hfq'-'gfp* transcripts. Hfq-GFP products were analyzed by SDS-PAGE. The relative level of polypeptide synthesis is shown at the bottom of each lane. The level of polypeptide synthesis in the absence of CsrA and Hfq was set to 100.

expression in the 1.5- to 10-fold range (11, 19, 27, 42, 43), it appears that CsrA functions in a fashion similar to a "governor" on a motor by reducing expression of some genes and increasing expression of others, rather than as an on-off switch.

A pwm search tool identified a potential CsrA binding site that overlaps the *hfq* SD sequence. The finding that this single site was similar to the SELEX-derived binding site consensus (Fig. 1) led us to investigate CsrA-dependent regulation of this gene. *hfq* is located in the *amiB-mutL-miaA-hfq-hflX* superoperon, which contains both $E\sigma^{32}$- and $E\sigma^{70}$-specific promoters (37, 38). Transcription of this operon is driven by at least five promoters during exponential growth (P_{mutL}, P_{miaA}, $P1_{hfq}$, $P2_{hfq}$, and $P3_{hfq}$). Our studies focused on the 68-nt mRNA leader originating from the SD sequence-proximal promoter, $P3_{hfq}$. Our gel shift (Fig. 2) and footprint (Fig. 3) results demonstrate that CsrA binds to the single site identified in silico. Moreover, the toeprint (Fig. 4) and cell-free translation (Fig. 7) results establish that bound CsrA inhibits Hfq synthesis by competitively blocking ribosome binding. While *hfq* mRNA contains only a single CsrA binding site, the affinity of the CsrA-*hfq* RNA interaction (K_d, 38 nM) is comparable to the affinity that CsrA has for mRNAs containing four to six binding sites (K_d, 22 to 40 nM). Despite the high affinity for *hfq* RNA, CsrA-mediated regulation was only 1.5- to 2-fold under our growth conditions (LB and LB plus glucose) (Fig. 5). This level of regulation is comparable to CsrA-dependent regulation of *cstA* expression in LB; however, regulation of *cstA* was ~5-fold in LB plus glucose (11). Thus, it is possible that growth conditions for optimum CsrA-dependent regulation of *hfq* were not achieved.

The finding that translational repression did not alter the stability of *hfq* mRNA constitutes the first example in which CsrA-mediated translational repression did not lead to accelerated mRNA decay (Fig. 6). The observation that CsrA did not influence the stability of *hfq* mRNA, combined with the finding that the steady-state level of *hfq* transcripts was elevated in *csrA* mutant strains, suggests that CsrA has a negative effect on *hfq* transcription as well as translation. While CsrA caused only a small reduction in expression of the *hfq'-'lacZ* fusion used in this study, it is important to note that our fusion contained only one of five known *hfq* promoters, $P3_{hfq}$. Since it is reasonable to assume that CsrA is capable of repressing translation initiation of transcripts derived from any of the *hfq* promoters, it appears likely that CsrA indirectly represses transcription from (at least) one of the other *hfq* promoters. Thus, the in vivo effect of CsrA on translation, as determined by the *hfq'-'lacZ* reporter, and the apparent indirect effect of CsrA on

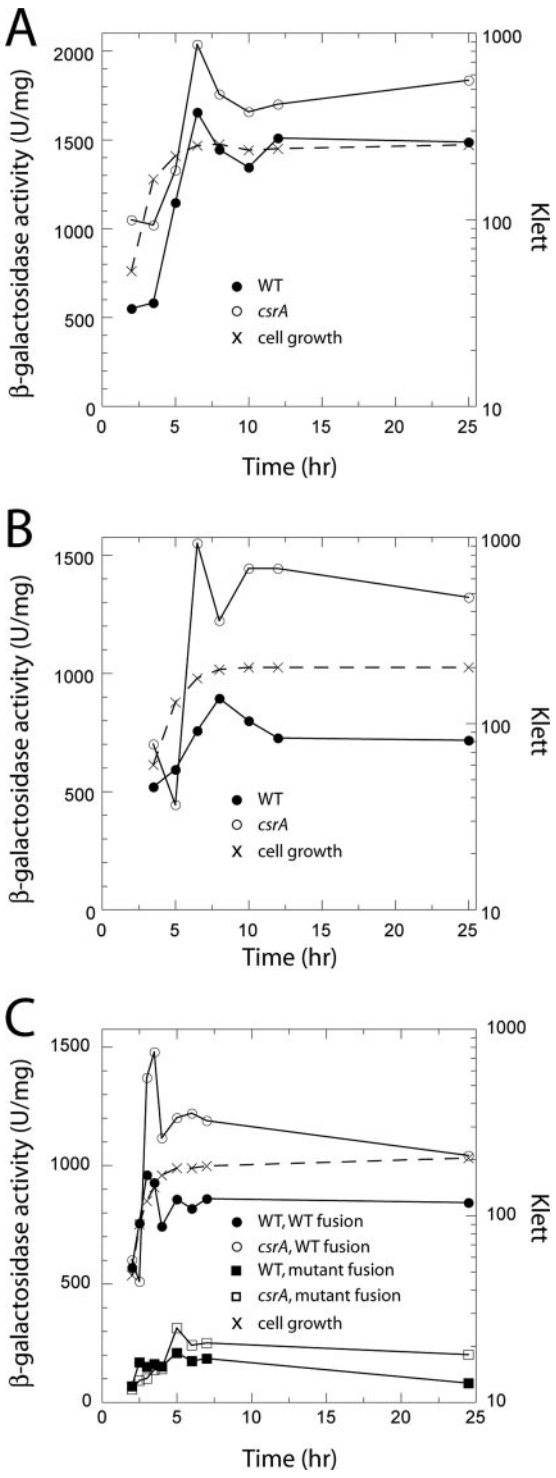

FIG. 6. CsrA-dependent regulation of an *hfq′-′lacZ* translational fusion. Cells were harvested at various times throughout growth and assayed for β-galactosidase activity. Growth medium was LB (A and B) or LB supplemented with 1% glucose (C). Growth curves for each strain in panels A, B, and C were essentially identical. The time shown is hours of cell growth. These experiments were conducted at least three times with similar results. Results from representative experiments are shown. (A) β-Galactosidase activity was determined for PLB785 (wild type [WT]) and PLB786 (*csrA::kan*). Cell growth was measured in strain PLB785. (B) β-Galactosidase activity was determined for PLB793 (*csrA::kan*/pCRA16 [WT]) and PLB789 (*csrA::kan*/pBR322 [*csrA*]). Cell growth was measured in strain PLB789. (C) β-Galactosidase activity was determined for PLB785 (WT, WT fusion), PLB786 (*csrA::kan* [*csrA*, WT fusion]), PLB923 (WT with mutant *hfq′-′lacZ* fusion), and PLB924 (*csrA::kan* [*csrA*] with mutant *hfq′-′lacZ* fusion). Cell growth was measured in strain PLB785.

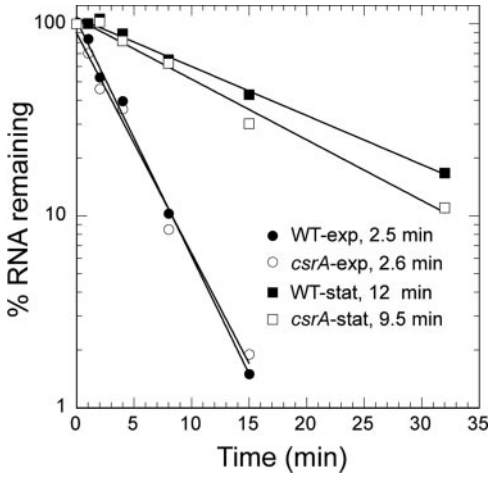

FIG. 7. Effects of growth phase and CsrA on *hfq* mRNA stability. *hfq* mRNA half-lives were determined in wild-type (WT) and *csrA* mutant strains during the exponential and early stationary phases of growth. The relative levels of mRNA remaining at 0, 1, 2, 4, 8, 15, and 32 min after the addition of rifampin were determined by RT-qRT-PCR. The mRNA level corresponding to each 0-min time point was set to 100. The mRNA half-life for each strain and growth phase is shown next to the corresponding symbol. Strains used were MG1655 (wild type) in exponential phase (WT-exp), TR1-MG1655 (*csrA::kan*) in exponential phase (*csrA*-exp), MG1655 in early stationary phase (WT-stat), and TR1-MG1655 in early stationary phase (*csrA*-stat).

hfq mRNA transcription, as determined by RT-qRT-PCR, likely contribute to the overall effect of CsrA on Hfq levels.

All previously characterized CsrA target mRNAs contain four or more CsrA binding sites (references 2, 11, 18, 42, and 45 and unpublished results). As CsrA is not a general repressor of translation, the finding that CsrA is capable of inhibiting translation of an mRNA containing a single CsrA binding site that overlaps its cognate SD sequence raises the question of how CsrA distinguishes one SD sequence from another. RNA secondary structure does not appear to be the only answer, as the majority of the known CsrA binding sites in mRNA targets, including the single binding site in *hfq*, do not contain their GGA motif in the loop of an RNA hairpin. Thus, additional conserved RNA sequence elements of binding sites must contribute to binding specificity.

Hfq is known to inhibit its own translation by binding to two sites within the *hfq* leader and initially translated region (41). Site A is located just upstream of the h1 hairpin, while binding site B overlaps its SD sequence (Fig. 3B). Both CsrA and Hfq are effective at inhibiting formation of a translation initiation complex. As Hfq-mediated autoregulation was reported to be about twofold, it is apparent that the level of CsrA-dependent and Hfq-dependent inhibition of *hfq* translation is similar. Moreover, it appears that CsrA-dependent and Hfq-depen-

dent inhibition of Hfq synthesis is additive despite the fact that the CsrA binding site and Hfq binding site B overlap (Fig. 5C).

Additional studies further establish an interrelationship between CsrA and Hfq. A global analysis of protein-protein interactions in *E. coli* using Hfq as the "bait" protein identified a stable interaction with CsrA (6). The intracellular levels of Hfq hexamers and CsrA dimers were determined to be approximately 9,000 and 16,000 molecules, respectively (14, 39). The mRNA signal intensity from a transcription profile of cells grown in minimal medium showed that the relative *hfq* transcript level (11,884) was comparable to that of *csrA* (7,783) (8). An additional study reported that Hfq stabilized RsmY RNA, a CsrB homolog in *Pseudomonas aeruginosa* (33). Moreover, that study suggested that RsmA, a CsrA homolog, and Hfq could bind concurrently to RsmY, a known antagonist of RsmA.

Csr and homologous Rsm systems have been identified in a wide variety of bacterial species (1, 26). Depending on the particular organism, this global regulatory system controls a variety of cellular processes and behaviors (e.g., RpoS stress signaling, quorum sensing, biofilm development, motility and chemotaxis, central carbon flux, and pathogenesis). The finding that the Csr circuitry is interconnected with other global regulatory networks suggests that Csr governs cellular behavior and physiology on a scale that is not yet fully understood.

ACKNOWLEDGMENTS

We thank Gisela Storz for Hfq, Ken Keiler for pETB, Emine Koc for technical assistance in the preparation of *E. coli* 30S ribosomal subunits, and Isaac Magaña for computer support.

This work was supported by Public Health Service grant GM59969 from the National Institutes of Health. Lél Eöry was supported in part by a fellowship from the Worldwide University Network.

REFERENCES

1. **Babitzke, P., and T. Romeo.** 2007. CsrB sRNA family: sequestration of RNA-binding regulatory proteins. Curr. Opin. Microbiol. **10:**156–163.
2. **Baker, C. S., I. Morozov, K. Suzuki, T. Romeo, and P. Babitzke.** 2002. CsrA regulates glycogen biosynthesis by preventing translation of *glgC* in *Escherichia coli*. Mol. Microbiol. **44:**1599–1610.
3. **Bevilacqua, J. M., and P. C. Bevilacqua.** 1998. Thermodynamic analysis of an RNA combinatorial library contained in a short hairpin. Biochemistry **37:** 15877–15884.
4. **Bolivar, F., R. L. Rodriguez, P. J. Greene, M. C. Betlach, H. L. Heyneker, and H. W. Boyer.** 1977. Construction and characterization of new cloning vehicles. II. A multipurpose cloning system. Gene **2:**95–113.
5. **Boyd, D., D. S. Weiss, J. C. Chen, and J. Beckwith.** 2000. Towards single-copy gene expression systems making gene cloning physiologically relevant: lambda InCh, a simple *Escherichia coli* plasmid-chromosome shuttle system. J. Bacteriol. **182:**842–847.
6. **Butland, G., J. M. Peregrín-Alvarez, J. Li, W. Yang, X. Yang, V. Canadien, A. Starostine, D. Richards, B. Beattie, N. Krogan, M. Davey, J. Parkinson, J. Greenblatt, and A. Emili.** 2005. Interaction network containing conserved and essential protein complexes in *Escherichia coli*. Nature **433:**531–537.
7. **Chenna, R., H. Sugawara, T. Koike, R. Lopez, T. J. Gibson, D. G. Higgins, and J. D. Thompson.** 2003. Multiple sequence alignment with the Clustal series of programs. Nucleic Acids Res. **31:**3497–3500.
8. **Corbin, R. W., O. Paliy, F. Yang, J. Shabanowitz, M. Platt, C. E. Lyons, Jr., K. Root, J. McAuliffe, M. I. Jordan, S. Kustu, E. Soupene, and D. F. Hunt.** 2003. Toward a protein profile of *Escherichia coli*: comparison to its transcription profile. Proc. Natl. Acad. Sci. USA **100:**9232–9237.
9. **Du, H., and P. Babitzke.** 1998. *trp* RNA-binding attenuation protein-mediated long distance RNA refolding regulates translation of *trpE* in *Bacillus subtilis*. J. Biol. Chem. **273:**20494–20503.
10. **Dubey, A. K., C. S. Baker, T. Romeo, and P. Babitzke.** 2005. RNA sequence and secondary structure participate in high-affinity CsrA-RNA interaction. RNA **11:**1579–1587.
11. **Dubey, A. K., C. S. Baker, K. Suzuki, A. D. Jones, P. Pandit, T. Romeo, and P. Babitzke.** 2003. CsrA regulates translation of the *Escherichia coli* carbon starvation gene, *cstA*, by blocking ribosome access to the *cstA* transcript. J. Bacteriol. **185:**4450–4460.
12. **Franze de Fernandez, M. T., L. Eoyang, and J. T. August.** 1968. Factor fraction required for the synthesis of bacteriophage Qβ-RNA. Nature **219:** 588–590.
13. **Gottesman, S.** 2004. The small RNA regulators of *Escherichia coli*: roles and mechanisms. Annu. Rev. Microbiol. **58:**303–328.
14. **Gudapaty, S., K. Suzuki, X. Wang, P. Babitzke, and T. Romeo.** 2001. Regulatory interactions of Csr components: the RNA binding protein CsrA activates *csrB* transcription in *Escherichia coli*. J. Bacteriol. **183:**6017–6027.
15. **Hartz, D., D. S. McPheeters, R. Traut, and L. Gold.** 1988. Extension inhibition analysis of translation initiation complexes. Methods Enzymol. **164:** 419–425.
16. **Jackson, D. W., K. Suzuki, L. Oakford, J. W. Simecka, M. E. Hart, and T. Romeo.** 2002. Biofilm formation and dispersal under the influence of the global regulator CsrA of *Escherichia coli*. J. Bacteriol. **184:**290–301.
17. **Kel, A. E., E. Gößling, I. Reuter, E. Cheremushkin, O. V. Kel-Margoulis, and E. Wigender.** 2003. MATCH^{TM}: a tool for searching transcription factor binding sites in DNA sequences. Nucleic Acids Res. **31:**3576–3579.
18. **Liu, M. Y., G. Gui, B. Wei, J. F. Preston III, L. Oakford, U. Yuksel, D. P. Giedroc, and T. Romeo.** 1997. The RNA molecule CsrB binds to the global regulatory protein CsrA and antagonizes its activity in *Escherichia coli*. J. Biol. Chem. **272:**17502–17510.
19. **Liu, M. Y., H. Yang, and T. Romeo.** 1995. The product of the pleiotropic *Escherichia coli* gene *csrA* modulates glycogen biosynthesis via effects on mRNA stability. J. Bacteriol. **177:**2663–2672.
20. **Livak, K. J., and T. D. Schmittgen.** 2001. Analysis of relative gene expression data using real-time quantitative PCR and the $2^{-\Delta\Delta CT}$ method. Methods **25:**402–408.
21. **Mondragon, V., B. Franco, K. Jonas, K. Suzuki, T. Romeo, Ö. Melefors, and D. Georgellis.** 2006. pH dependent activation of the BarA-UvrY two-component system in *Escherichia coli*. J. Bacteriol. **188:**8303–8306.
22. **Moody, E. M., J. C. Feerrar, and P. C. Bevilacqua.** 2004. Evidence that folding of an RNA tetraloop hairpin is less cooperative than its DNA counterpart. Biochemistry **43:**7992–7998.
23. **Muffler, A., D. Fischer, and R. Hengge-Aronis.** 1996. The RNA-binding protein HF-1 plays a global regulatory role which is largely, but not exclusively, due to its role in expression of the sigma(s) subunit of RNA polymerase in *Escherichia coli*. J. Bacteriol. **179:**297–300.
24. **Platt, T., B. Müller-Hill, and J. H. Miller.** 1972. Assay of β-galactosidase, p. 352–355. *In* J. H. Miller (ed.), Experiments in molecular genetics. Cold Spring Harbor Laboratory Press, Cold Spring Harbor, NY.
25. **Remold-O'Donnell, E., and R. E. Thach.** 1970. A new method for the purification of initiation factor F2 in high yield, and an estimation of stoichiometry in the binding reaction. J. Biol. Chem. **245:**5737–5742.
26. **Romeo, T.** 1998. Global regulation by the small RNA-binding protein CsrA and the non-coding RNA molecule CsrB. Mol. Microbiol. **29:**1321–1330.
27. **Romeo, T., M. Gong, M. Y. Liu, and A.-M. Brun-Zinkernagel.** 1993. Identification and molecular characterization of *csrA*, a pleiotropic gene from *Escherichia coli* that affects glycogen biosynthesis, gluconeogenesis, cell size, and surface properties. J. Bacteriol. **175:**4744–4755.
28. **Sabnis, N. A., H. Yang, and T. Romeo.** 1995. Pleiotropic regulation of central carbohydrate metabolism in *Escherichia coli* via the gene *csrA*. J. Biol. Chem. **270:**29096–29104.
29. **Sauter, C., J. Basquin, and D. Suck.** 2003. Sm-like proteins in eubacteria: the crystal structure of the Hfq protein from *Escherichia coli*. Nucleic Acids Res. **32:**4091–4098.
30. **Schaak, J. E., H. Yakhnin, P. C. Bevilacqua, and P. Babitzke.** 2003. A Mg_2^+-dependent RNA tertiary structure forms in the *Bacillus subtilis trp* operon leader transcript and appears to interfere with *trpE* translation control by inhibiting TRAP binding. J. Mol. Biol. **332:**555–574.
31. **Schultz, J. E., and A. Matin.** 1991. Molecular and functional characterization of a carbon starvation gene of *Escherichia coli*. J. Mol. Biol. **218:**129–140.
32. **Silhavy, T. J., M. L. Berman, and L. W. Enquist.** 1984. Experiments with gene fusions. Cold Spring Harbor Laboratory Press, Cold Spring Harbor, NY.
33. **Sorger-Domenigg, T., E. Sonnleitner, V. R. Kaberdin, and U. Bläsi.** 2007. Distinct and overlapping binding sites of *Pseudomonas aeruginosa* Hfq and RsmA proteins on the non-coding RNA RsmY. Biochem. Biophys. Res. Commun. **352:**769–773.
34. **Storz, G., J. A. Opdyke, and A. Zhang.** 2004. Controlling mRNA stability and translation with small, noncoding RNAs. Curr. Opin. Microbiol. **7:**140–144.
35. **Suzuki, K., P. Babitzke, S. R. Kushner, and T. Romeo.** 2006. Identification of a novel regulatory protein (CsrD) that targets the global regulatory RNAs CsrB and CsrC for degradation by RNase E. Genes Dev. **20:**2605–2617.
36. **Suzuki, K., X. Wang, T. Weilbacher, A. K. Pernestig, Ö. Melefors, D. Georgellis, P. Babitzke, and T. Romeo.** 2002. Regulatory circuitry of the CsrA/CsrB and BarA/UvrY systems of *Escherichia coli*. J. Bacteriol. **184:** 5130–5140.
37. **Tsui, H. C., G. Feng, and M. E. Winkler.** 1996. Transcription of the *mutL* repair, *miaA* tRNA modification, *hfq* pleiotropic regulator, and *hflA* region protease genes of *Escherichia coli* K-12 from clustered σ^{32}-specific promoters during heat shock. J. Bacteriol. **178:**5719–5731.
38. **Tsui, H. C., H. C. Leung, and M. E. Winkler.** 1994. Characterization of

broadly pleiotropic phenotypes caused by an *hfq* insertion mutation in *Escherichia coli* K-12. Mol. Microbiol. **13:**35–49.

39. **Valentin-Hansen, P., M. Eriksen, and C. Udesen.** 2004. The bacterial Sm-like protein Hfq: a key player in RNA transactions. Mol. Microbiol. **51:**1525–1533.
40. **Vasil'eva, I. M., and M. B. Garber.** 2002. The regulatory role of the Hfq protein in bacterial cells. Mol. Biol. **36:**785–791.
41. **Vecerek, B., I. Moll, and U. Bläsi.** 2005. Translational autocontrol of the *Escherichia coli hfq* RNA chaperone gene. RNA **11:**976–984.
42. **Wang, X., A. K. Dubey, K. Suzuki, C. S. Baker, P. Babitzke, and T. Romeo.** 2005. CsrA post-transcriptionally represses *pgaABCD*, responsible for synthesis of a biofilm polysaccharide adhesin of *Escherichia coli*. Mol. Microbiol. **56:**1648–1663.
43. **Wei, B. L., A. M. Brun-Zinkernagel, J. W. Simecka, B. M. Prüß, P. Babitzke, and T. Romeo.** 2001. Positive regulation of motility and *flhDC* expression by the RNA-binding protein CsrA of *Escherichia coli*. Mol. Microbiol. **40:**245–256.
44. **Wei, B. L., S. Shin, D. LaPorte, A. J. Wolfe, and T. Romeo.** 2000. Global regulatory mutations in *csrA* and *rpoS* cause severe central carbon stress in *Escherichia coli* in the presence of acetate. J. Bacteriol. **182:**1632–1640.
45. **Weilbacher, T., K. Suzuki, A. K. Dubey, X. Wang, S. Gudapaty, I. Morozov, C. S. Baker, D. Georgellis, P. Babitzke, and T. Romeo.** 2003. A novel sRNA component of the carbon storage regulatory system of *Escherichia coli*. Mol. Microbiol. **48:**657–670.
46. **Yakhnin, A. V., J. J. Trimble, C. R. Chiaro, and P. Babitzke.** 2000. Effects of mutations in the L-tryptophan binding pocket of the *trp* RNA-binding attenuation protein of *Bacillus subtilis*. J. Biol. Chem. **275:**4519–4524.
47. **Yakhnin, H., H. Zhang, A. V. Yakhnin, and P. Babitzke.** 2004. The *trp* RNA-binding attenuation protein of *Bacillus subtilis* regulates translation of the tryptophan transport gene *trpP* (*yhaG*) by blocking ribosome binding. J. Bacteriol. **186:**278–286.
48. **Yang, H., M. Y. Liu, and T. Romeo.** 1996. Coordinate genetic regulation of glycogen catabolism and biosynthesis in *Escherichia coli* via the CsrA gene product. J. Bacteriol. **178:**1012–1017.
49. **Zuker, M.** 2003. Mfold web server for nucleic acid folding and hybridization prediction. Nucleic Acids Res. **31:**3406–3415.